

1 **Enhanced BCR signalling inflicts early plasmablast and germinal centre B**
2 **cell death**

3 Yam-Puc JC^{1*}, Zhang L¹, Maqueda-Alfaro RA², Garcia-Ibanez L¹, Zhang Y¹, Davies J¹, Senis
4 YA³, Snaith M⁴ and Toellner KM^{1*}.

5 ¹Institute of Immunology and Immunotherapy, College of Medical & Dental Sciences,
6 University of Birmingham, Birmingham, B15 2TT, UK.

7 ²Center for Advanced Research, The National Polytechnic Institute, Cinvestav-IPN, Mexico
8 City, 07340, Mexico.

9 ³ Université de Strasbourg, Institut National de la Santé et de la Recherche Médicale,
10 Etablissement Français du Sang Grand Est, Unité Mixte de Recherche-S 1255, Fédération de
11 Médecine Translationnelle de Strasbourg, Strasbourg, France

12 ⁴AstraZeneca Medimmune Cambridge, Antibody Discovery and Protein Engineering,
13 Cambridge, UK.

14

15 ***Corresponding authors:**

16 Kai-Michael Toellner / Juan Carlos Yam-Puc
17 Institute of Immunology and Immunotherapy
18 College of Medical & Dental Sciences/IBR
19 University of Birmingham
20 Birmingham B15 2TT
21 United Kingdom
22 E-mail: k.m.toellner@bham.ac.uk / j.c.yam-puc@bham.ac.uk
23 Phone: +44 121 415 8681, Fax: +44 121 441 43599

24 **Abstract**

25 It is still not clear how B-cell receptor (BCR) signalling intensity affects plasma cell and
26 germinal centre (GC) B cell differentiation. We generated $C\gamma 1^{Cre/+}Ptpn6^{fl/fl}$ mice where SHP-1,
27 a negative regulator of BCR signalling, is deleted rapidly after B cell activation. Although
28 immunisation with T-dependent antigens increased BCR signalling, it led to plasma cells
29 reduction and increased apoptosis. Dependent on the antigen, the early GC B cell response
30 was equally reduced and apoptosis increased. At the same time, a higher proportion of GC B
31 cells expressed cMYC, indicating increased GC B cell – Tfh cell interactions. While GC B cell
32 numbers returned to normal at later stages, affinity maturation was suppressed in the long term.
33 This confirms that BCR signalling not only directs affinity dependent B cell selection but also,
34 without adequate Tfh cell help, can inflict cell death, which may be important for the
35 maintenance of B cell tolerance.

36

37 **Key words.** B cell receptor signalling, plasma cells, SHP-1, apoptosis, hyper-active state,
38 class-switch recombination, tolerance, affinity maturation

39 **Introduction**

40 Specific interaction between antigen and the B-cell receptor (BCR) is the key signal for B cell
41 selection and activation (Niiro and Clark, 2002; Yam-Puc et al., 2018). After initial activation
42 *in vivo*, B cells may differentiate into plasma cells (PCs) through rapid extra-follicular
43 expansion or become germinal centre (GC) cells that will undergo BCR affinity maturation for
44 antigen (MacLennan, 1994; MacLennan et al., 2003; Victora and Nussenzweig, 2012). GCs
45 contribute to long-lived humoral responses by producing high-affinity antibody-forming PCs
46 and memory B cells (MacLennan, 1994; Victora and Nussenzweig, 2012; Weisel et al., 2016).
47 High affinity neutralising antibodies represent a crucial mechanism by which vaccines or
48 natural infections confer sterilising immunity protecting against on re-exposure to the same
49 pathogen (Bachmann et al., 1994; Steinhoff et al., 1995). Two major signals regulate B cell
50 activation leading to antibody production: while signals from T helper cells have been studied
51 intensely in recent years (Oropallo and Cerutti, 2014; Shulman et al., 2013; Victora et al.,
52 2010), less attention has been given to the impact of BCR signalling during selection of B cells
53 by antigen (Khalil et al., 2012; Mueller et al., 2015). The interaction between antigen and BCR
54 controls whether activated B cells entering the GC or undergo rapid PC differentiation in extra-
55 follicular proliferative foci. B cell clones undergoing a strong initial interaction with antigen
56 can efficiently differentiate into extra-follicular PCs contributing to the rapid early phase of the
57 antibody production (Paus et al., 2006). B cells expressing a wide range of BCR affinities
58 become pre-GC B cells after T-B interaction (Dal Porto et al., 2002; Schwickert et al., 2011;
59 Victora et al., 2010). Higher affinity BCRs can induce stronger signal transduction than lower
60 affinity ones (Kouskoff et al., 1998). BCR occupancy is a product of BCR affinity and antigen
61 concentration, and concentration of free antigen can be limited by antibody feedback (Toellner
62 et al., 2018). The effect of all of this on cell fate decisions during B cell differentiation merits
63 more attention.

64 The Src homology 2 (SH2) domain-containing protein-tyrosine phosphatase (PTP)-1 (SHP-1),
65 encoded by the *Ptpn6* gene, negatively regulates BCR signalling primarily via its binding to
66 the immunoreceptor tyrosine-based inhibitory motif (ITIM)- containing receptors CD72,
67 CD22, FcγRIIB and paired Ig-like receptor (PIR)-B (Adachi et al., 2001; D'Ambrosio et al.,
68 1995; Maeda et al., 1998; Nitschke and Tsubata, 2004). SHP-1 is expressed and constitutively
69 activated in all B cells and its specific deletion on B cells results in systemic autoimmunity
70 (Pao et al., 2007). SHP-1 is highly expressed and activated in GC B cells, suggesting that BCR
71 signalling is negatively regulated during differentiation of GC B cells (Khalil et al., 2012).
72 While BCR signalling has been shown to be absent in dark zone (DZ) GC B cells (Stewart et
73 al., 2018), there is more signal transduction in light zone (LZ) B cells competing for selection
74 signals through affinity-dependent activation of their BCR (Mueller et al., 2015).

75 In order to test how BCR signalling inhibition by SHP-1 affects antigen-induced B cell
76 differentiation, we generated $C\gamma 1^{Cre/+}Ptpn6^{fl/fl}$ mice, in which the T-dependent B cell activation
77 induces SHP-1 deletion in most B cells (Roco et al., 2019). Most induction of immunoglobulin
78 class switch recombination (CSR) happens during the initial phase of cognate T cell - B cell
79 interaction before GCs are formed (Marshall et al., 2011; Roco et al., 2019; Toellner et al.,
80 1998; Zhang et al., 2016). Using this system, we show that $C\gamma 1^{Cre/+}Ptpn6^{fl/fl}$ B cells exhibit
81 stronger BCR signalling. Paradoxically this leads to a smaller extra-follicular IgG1⁺ PC
82 response and to death of GC B cells, resulting in reduced affinity maturation in the GC.

83 **Results**

84 **Increased apoptosis in extra-follicular plasma cells of $C\gamma 1^{Cre/+}Ptpn6^{fl/fl}$ mice**

85 B cells binding antigen with higher affinity are more likely to differentiate into extra-follicular
86 PCs (O'Connor et al., 2006; Paus et al., 2006). To test whether deletion of the negative regulator
87 of BCR signalling, SHP-1, affects the early extra-follicular PC response to immunisation,

88 $C\gamma 1^{Cre/+}Ptpn6^{fl/wt}$ and $C\gamma 1^{Cre/+}Ptpn6^{fl/fl}$, in the following abbreviated as $Shp1^{fl/wt}$ and $Shp1^{fl/fl}$
89 mice, were immunised with SRBCs i.v.. The $C\gamma 1^{Cre}$ allele reports expression of IgG1 germline
90 transcripts (Casola et al., 2006). These are strongly induced after the initial interaction of B
91 cells with T helper cells before PCs or GCs appear (Marshall et al., 2011; Roco et al., 2019;
92 Zhang et al., 2018). This should lead to efficient deletion of SHP-1 in extra-follicular PCs and
93 GC founder B cells. Spleens were analysed 5 days post immunisation, when the extra-follicular
94 PC response peaks and early GCs have formed (Zhang et al., 2018).

95 Against expectation, flow cytometry showed that PC numbers were reduced by 50% in $Shp1^{fl/fl}$
96 mice (Fig. 1A). This primarily affected IgG1 switched PCs, while non-switched IgM PCs
97 developed in similar numbers as in $Shp1^{fl/wt}$ control animals (Fig. 1B). Immunohistology, using
98 IRF4 as a marker for PCs, showed reduced PC foci in the splenic red pulp, primarily in the
99 IgG1-switched PCs of $Shp1^{fl/fl}$ mice (Fig. 1C). PCs emerging from GCs at the GC-T zone
100 interface (GTI) (Zhang et al., 2018) were unaffected at this point (Supp. Fig. 1). Taken together,
101 these data indicate that increased BCR signalling after initial B cell activation inhibits extra-
102 follicular PC differentiation.

103 Hyper-activation of B cells through BCR signalling can lead to programmed cell death (Akkaya
104 et al., 2018; Parry et al., 1994; Tsubata et al., 1994a; Tsubata et al., 1994b; Watanabe et al.,
105 1998). In order to test whether cell death was responsible for the smaller extra-follicular PC
106 response, apoptotic cells were detected using Annexin V and 7-AAD staining. This showed an
107 increase in the proportion of apoptotic PCs (Annexin V^{+ve} and 7-AAD^{+ve}) in $Shp1^{fl/fl}$ mice (Fig.
108 2A). Furthermore, the expression of active caspase-3 on different isotypes of PCs showed that
109 both IgG1⁺ and to some extent IgM⁺ PCs of $Shp1^{fl/fl}$ animals were more likely to express active
110 caspase-3 (Fig. 2B). Immunohistology confirmed an increase in active caspase-3⁺ cells in the
111 IRF-4⁺ extra-follicular splenic foci of $Shp1^{fl/fl}$ mice (Fig. 2C). While the increase in apoptosis
112 appears to be relatively small (+20%), it is worth mentioning that cells at this late stage of

113 apoptosis are rapidly removed (Hanayama et al., 2004). Therefore, this likely underestimates
114 the amount of apoptosis at this specific stage of the response, indicating that an inappropriate
115 increase in BCR signalling can negatively affect extra-follicular PC generation through
116 increased cell death.

117 **SRBC induced GCs of Shp1^{fl/fl} mice are largely unaffected**

118 In established GCs, BCR signalling is limited by SHP-1 hyper-phosphorylation, and this is
119 important for GC maintenance (Khalil et al., 2012). In order to test how SHP-1 deletion,
120 starting from the earliest stages of GC development, affects the GC response we followed GC
121 B cell differentiation in $C\gamma 1^{Cre/+}Ptpn6^{fl/fl}$ mice 5 d after SRBC immunisation. Surprisingly, at
122 this early stage there was no significant change in the number of GC B cells in Shp1^{fl/fl} mice
123 (Fig. 3A). Flow cytometry confirmed a reduction of SHP-1 staining intensity in all GC B cells
124 (Supp. Fig. 2A), indicating most GC B cells successfully deleted the gene. The increased in
125 SYK phosphorylation seen in GC B cells in Shp1^{fl/fl} mice confirmed that SHP-1 deletion does
126 increase BCR signalling in this system (Fig. 3B). In contrast to what was seen in extra-follicular
127 PCs, cell death in GC B cells, evaluated by flow cytometric analysis of Annexin V / 7-AAD
128 and active caspase 3 staining, was not increased at this stage (Fig 3C).

129 **Germinal centre B cell responses and affinity maturation to NP-CGG are impaired in** 130 **$C\gamma 1^{Cre/+}Ptpn6^{fl/fl}$ mice**

131 While SRBC immunisation rapidly induces B cell activation and differentiation (Zhang et al.,
132 2018), it also has a substantial T independent component and therefore is not necessarily the
133 strongest inducer of IgG1 germline transcription. Protein antigens in alum induce strong Th2
134 type B cell activation, IL-4 expression in T cells, and rapid extra-follicular PCs as well as GC
135 differentiation in draining lymph nodes (Toellner et al., 1998).

136 Eight days post s.c. immunisation with NP-CGG, *Shp1^{fl/fl}* draining lymph nodes showed a
137 similar level of PC reduction than in *Shp1^{fl/fl}* spleens after SRBC immunisation. GC B cells
138 were also reduced (Fig. 4A, B). Again, SHP-1 deletion (Supp. Fig. 2B) resulted in increased
139 BCR signalling, as detected by increased SYK phosphorylation (Fig. 4C). Further, cMYC
140 expression, induced after GC B cell interaction with Tfh cells (Calado et al., 2012; Dominguez-
141 Sola et al., 2012; Luo et al., 2018), was increased in *Shp1^{fl/fl}* GC B cells (Fig. 4D), suggesting
142 also more efficient T-dependent B cell activation. Despite this, apoptosis in GC B cells was
143 increased (Fig. 4E). Deletion of C-terminal Src kinase (CSK), another downstream inhibitor of
144 BCR signalling, led to a similar reduction of the GC B cell response in *Cγ1^{Cre/+}CSK^{fl/fl}* mice
145 after NP-CGG immunisation (Supp. Fig. 3).

146 In order to test the effects of SHP-1 deletion on later stages of the response to TD antigens, the
147 splenic GC response and affinity maturation were monitored after intraperitoneal immunisation
148 of *Shp1^{fl/fl}* and *Shp1^{fl/wt}* mice with NP-CGG. Similar to the early GC response in lymph nodes,
149 increased BCR signalling led to a reduced splenic GC response by day 8 after immunisation,
150 but this effect was lost at later stages of the response (Fig. 4F). As expected, antigen-specific
151 IgM production was unaffected, and NP-specific IgG1 was marginally reduced at the earliest
152 stages of the response. At later stages, however, there was no difference in antibody titre and
153 after 14 d after immunization *Shp1^{fl/fl}* mice did not further increase affinity of NP-specific
154 serum IgG (Fig. 4G), showing that despite the normalization in cell numbers, there is a long-
155 term effect on the efficiency of affinity dependent B cell selection.

156 **Discussion**

157 During development B cells are strictly selected for the continuous expression of a functional
158 BCR and the loss of its expression leads to rapid cell death (Kraus et al., 2004; Lam et al.,
159 1997). Altering the expression of downstream signalling molecules changes the BCR signalling

160 strength which in turn affects B cell development, (Cariappa et al., 2001; Nguyen et al., 2017;
161 Pao et al., 2007; Tsiantoulas et al., 2017). For example, enhanced BCR signalling due to
162 specific deletion of SHP-1 in all B cells leads to B1a B cell subset expansion (Pao et al., 2007).
163 The effect of altering BCR signalling strength also depends on the phase of development.
164 Enhanced BCR signalling in transitional B cells favours follicular B cell development
165 (Cariappa et al., 2001). Few studies have tested the effects of artificially enhanced BCR
166 signalling in mature B cells that had undergone normal B cell development (Davidzohn et al.,
167 2020; Li et al., 2014). The model presented here allows normal B cell development and
168 increased BCR signalling by deletion of SHP-1 only after mature and naïve B cells are activated
169 by signals that may induce class-switching to IgG1.

170 In mature naïve B cells, antigen binding induces a cascade of phosphorylation involving the
171 accessibility of immunoreceptor tyrosine-based activation motifs (ITAMs) on I α (CD79A)
172 and I β (CD79B), leading to activation of key molecules to finally activate transcription factors
173 and prompt an immune response (Buchner and Muschen, 2014). SHP-1 inhibits BCR signalling
174 through SYK (Adachi et al., 2001), and activated B cells in the current model show clear signs
175 of pSYK overexpression after B cell activation.

176 After antigen mediated BCR stimulation and T cell help, B cells may differentiate into extra-
177 follicular PCs (MacLennan et al., 2003) or become GC precursor cells to start GC reactions
178 (MacLennan, 1994; Victora and Nussenzweig, 2012). The exact mechanisms which control the
179 differentiation of B cells into extra-follicular PCs or GCs is still controversial and under
180 scrutiny. It has been shown that B cells experiencing a strong initial interaction with antigen
181 more efficiently differentiate into extra-follicular PCs (Paus et al., 2006). Here, we show that
182 higher signalling through the BCR affects PC differentiation in unexpected ways. C γ 1 germline
183 transcripts are induced during the initial B cell activation prior to extra-follicular or GC B cell

184 differentiation (Marshall et al., 2011; Roco et al., 2019). Therefore, early B blasts
185 differentiating into extra-follicular plasmablasts would be the first to encounter Cre mediated
186 deletion of SHP-1 and increased BCR signalling. As increased BCR signalling should enhance
187 extra-follicular PC differentiation (Paus et al., 2006), it was surprising to see reduced numbers
188 of extra-follicular plasmablasts. Due to the low number of B cells activated in a non-BCR
189 transgenic animal it was not possible to test whether the number of B cells initially activated
190 to enter plasmablast differentiation was changed. Stronger BCR mediated activation may well
191 have led to larger numbers of B cells entering plasmablast differentiation, however, stronger
192 activation in the absence of co-stimulation from T cells can also induce activation-induced cell
193 death (Akkaya et al., 2018; Parry et al., 1994; Tsubata et al., 1994a; Tsubata et al., 1994b;
194 Watanabe et al., 1998). This would suggest that after activation, SHP-1-deficient B cells are
195 not maintained since they do not receive timely co-stimulatory signals needed for full activation
196 (Akkaya et al., 2018). These results are in line with data from an earlier study (Li et al., 2014)
197 that showed a modest reduction in PC production in the response to primary immunisation with
198 TD antigens in mice where *Ptpn6* is deleted by Cre expressed under the control of the *Aicda*
199 promoter (Li et al., 2014). *Aicda* is also induced during primary B cell activation before GCs
200 form, however, its expression starts slightly later and at lower levels than *Cy1* germline
201 transcripts (Roco et al., 2019), which may explain the more subtle changes.

202 The effect of SHP-1 deletion on GC size is only transient which could be due to the expansion
203 of a minority of cells with incomplete deletion. The longer-term change in affinity maturation,
204 however, makes it more likely that the complex balance between affinity dependent GC B cell
205 selection, proliferation, output, and death reaches a new equilibrium, filling GC B cell niches
206 to normal occupancy levels. This may explain differences seen to an earlier study, where
207 tamoxifen-induced deletion of SHP-1 during the peak of the GC response resulted in a rapid
208 loss of GC B cells within a short period (Khalil et al., 2012).

209 Although the effect on the size of the GC compartment in NP-CGG immunised mice was only
210 transient, the higher pSYK levels clearly indicate considerably increased signal transduction in
211 GC B cells. pSYK levels were also increased in GC B cells induced by SRBC immunization,
212 although there was less obvious effect on GC size. This may be explainable by the fact that the
213 response to SRCB immunisation is less dependent on T cell help, and that GC B cells are able
214 to survive and expand for a limited time without T cell help (de Vinuesa et al., 2000). A recent
215 study testing the inhibition of pSYK degradation in GC B cells using mixed bone marrow
216 chimeras (Davidzohn et al., 2020) showed that increased SYK signalling led to an increase in
217 the GC LZ compartment. Further differentiation of these LZ B cells depended on Tfh cell help
218 (Davidzohn et al., 2020; de Vinuesa et al., 2000; Gitlin et al., 2015; Shulman et al., 2013). We
219 show here that SHP-1 deletion in the GC leads to higher levels of pSYK. At least some of these
220 GC B cells are able to recruit efficient Tfh cell help, indicated by the increased expression of
221 cMYC (Calado et al., 2012; Dominguez-Sola et al., 2012). However, many early GC B cells
222 undergo apoptosis, possibly because Tfh cell help is limiting at this early stage. GCs are not
223 only sites of affinity maturation. B cell selection in the GC also guarantees peripheral tolerance
224 (Goodnow et al., 1989; Russell et al., 1991). The data shown here could reflect the deletion of
225 autoreactive GC B cells that encounter inadequate BCR signalling and are not able to recruit
226 adequate Tfh cell help in time. In the same way, higher affinity SHP1-deficient GC B cells may
227 be deleted because they are not recruiting sufficient Tfh cell help. This would indicate that
228 affinity dependent BCR signalling not only is important for affinity dependent B cell selection,
229 but also that the balance of BCR signalling and Tfh cell-mediated rescue may regulate tolerance
230 during the GC B cell responses.

231 **Author Contributions**

232 Conceptualization, J.C.Y-P. and K.M.T. Investigation, J.C.Y.P., L.Z., R.A.M-A., L.G-I., Y.Z.
233 Formal analysis J.C.Y-P. Resources, Y.A.S., M.S and K.M.T. Writing – Original Draft, J.C.Y-

234 P. Writing – Review & Editing, J.C.Y-P. and K.M.T. All authors reviewed and edited the final
235 version of the manuscript. Supervision and Funding Acquisition, K.M.T.

236 **Acknowledgments**

237 We are grateful to Benjamin G. Neel (NYU School of Medicine) for $Ptpn6^{fl/wt}$ mice and S.
238 Casola (IFOM, Milan, Italy) for $Cy1^{Cre/+}$ mice. We thank Mark J. Shlomchik and Wei Luo for
239 helpful discussion. In addition, we would like to thank at the Biomedical Service Unit, Flow
240 Cytometry Services and Microscopy and Imaging Services at the University of Birmingham.
241 This work was supported by grants from the BBSRC BB/M025292/1 to K.M.T., post-doctoral
242 fellowship program from National Council of Science and Technology-Mexico (CONACYT-
243 Mexico) to J.C.Y-P.

244 **Conflict of Interest Statement**

245 The authors declare no personal, professional or financial conflict of interest.

246 **Figure Legends**

247 **Figure 1. Plasma cells are reduced in $Cy1^{Cre/+}Ptpn6^{fl/fl}$ mice post SRBCs immunisation.**

248 Mice spleens were analysed 5 days post immunisation with SRBCs **A.** Representative contour
249 plots gating PCs (lymphocytes/singlets/live/B220⁻CD138⁺). Right: Summary data (% of live
250 cells; data combined from three independent experiments. WT, n=11; Shp1, n=17). **B.**
251 Percentage of IgM⁺ and IgG1⁺ PCs (% of live cells; data combined from three independent
252 experiments. WT, n=11; Shp1, n=17) **C.** Splenic sections from $Shp1^{fl/wt}$ (fl/wt) and $Shp1^{fl/fl}$
253 (fl/fl) mice staining B cell follicles (IgD, green), T cell zone (CD4, blue) and PCs (top, IRF4 in
254 red), or IgG1⁺ cells (bottom, IgG1 in red), scale bar 200 μ m. Positive area of IRF4 and IgG1
255 was calculated as percentage of total splenic area. Data are representative of one of two

256 independent experiments, WT, n=4; Shp1, n=5. Horizontal lines indicate the mean. *P < 0.05,
257 **P < 0.01 (parametric two-tailed unpaired t-test).

258 **Figure 2. Plasma cell apoptosis is increased in SRBC immunised $C\gamma 1^{Cre/+}Ptpn6^{fl/fl}$ mice.**

259 Apoptosis rate on PCs was analysed 5 days post SRBCs immunisation in $C\gamma 1^{Cre/+}Ptpn6^{fl/wt}$
260 (*fl/wt*) and $C\gamma 1^{Cre/+}Ptpn6^{fl/fl}$ (*fl/fl*) mice. **A.** Representative dot plots show apoptosis rate based
261 on the binding of Annexin V and the dead cell dye 7-AAD (pregated on PCs; top panel).
262 Annexin V⁺ 7-AAD⁻ cells were considered as early apoptotic cells and Annexin V⁺ 7-AAD⁺
263 cells as late apoptotic cells. Summary data (bottom panel; % of plasma cells; results are
264 combined from two independent experiments. WT, n=7; Shp1, n=10. **B.** Active caspase-3
265 expression on IgG1⁺ or IgM⁺ PCs. Graphs on the right show summary of data as percentage of
266 active caspase-3⁺ cells (% of plasma cells; results are combined from three independent
267 experiments. WT, n=11; Shp1, n=17). **C.** Spleen sections from $Shp1^{fl/wt}$ (*fl/wt*) and $Shp1^{fl/fl}$
268 (*fl/fl*) mice staining for B cell follicles (IgD, green), T cell zone (CD4, blue) and PCs (IRF4 in
269 red) in the top, or active caspase-3⁺ cells (Caspase-3 in red) in the bottom. Ratio of active
270 caspase 3⁺ pixel / IRF4⁺ pixel, representative of one of two independent experiments. WT, n=4;
271 Shp1, n=5. Horizontal lines indicate the mean. *P < 0.05, ***P < 0.01 (parametric two-tailed
272 unpaired t-test).

273 **Figure 3. SRBC induced GCs of $C\gamma 1^{Cre/+}Ptpn6^{fl/fl}$ mice are largely unaffected.** Germinal

274 centre response was analysed 5 days post SRBC immunisation of $C\gamma 1^{Cre/+}Ptpn6^{fl/wt}$ (*fl/wt*) and
275 $C\gamma 1^{Cre/+}Ptpn6^{fl/fl}$ (*fl/fl*) mice. **A.** Representative contour plots gating GC B cells from spleen
276 (lymphocytes/singlets/live/CD138⁻B220⁺CD38⁻Fas⁺). Right panel shows summary of data (%
277 of B220⁺ B cells; data are combined from two independent experiments. WT, n=8; Shp1,
278 n=12). **B.** pSYK expression in GC B cells. Right panel shows summary data (median
279 fluorescence intensity (MFI) of GC B cells; results are representative of two independent
280 experiments. WT, n=4; Shp1, n=5). **C.** Apoptosis rate based on the binding of Annexin V and

281 7-AAD, active caspase-3 in IgG1⁺ or IgM⁺ cells as in Figure 2. (% of GC B cells; data are
282 combined from two independent experiments. WT, n=7; Shp1, n=10) horizontal lines indicate
283 the mean. *P < 0.05 (parametric two-tailed unpaired t-test).

284 **Figure 4. Germinal centre B cell responses and affinity maturation to NP-CGG are**
285 **impaired in C γ 1^{Cre/+}Ptpn6^{fl/fl} mice.** **A)** Germinal centre B cell responses in popliteal lymph
286 nodes (PLN) d8 post NP-CGG immunisation of C γ 1^{Cre/+}Ptpn6^{fl/wt} (*fl/wt*) mTmG and
287 C γ 1^{Cre/+}Ptpn6^{fl/fl} (*fl/fl*) mTmG mice. Sequential gating strategy for identification of PCs
288 (lymphocytes/singlets/live/tomato⁻GFP⁺B220⁻CD138⁺) and GC B cells
289 (lymphocytes/singlets/live/tomato⁻GFP⁺CD138⁻B220⁺CD38⁻Fas⁺). **B.** Summary data of PCs
290 and GC cells (% of live cells; three independent experiments; WT, n=15; Shp1, n=11). **C.** SYK
291 phosphorylation in GC B cells from PLN 8 days post NP-CGG immunisation (MFI on GC B
292 cells; representative results from one of two independent experiments. WT, n=5; Shp1, n=4).
293 **D.** Summary data of relative percentage of GC cMYC expression measured from stained PLN
294 sections 8 days post NP-CGG immunisation. (Each dot represents a different GC. Data
295 combined from two independent experiments. WT, n=8; Shp1, n=10). **E.** Active caspase-3 on
296 GC B cells from PLNs 8 days post NP-CGG immunisation (% of GC B cells; results are
297 representative of one of two independent experiments. WT, n=5; Shp1, n=4). **F.** Splenic NP-
298 specific GC B cells at different time points after immunisation (% of live cells; results are from
299 one to two independent experiments at each time-point. WT, n=4-8; Shp1, n=3-8). **G.** Serum
300 antibody titres for NP-specific IgM (left panel, WT, n=4-8; Shp1, n=3-8), IgG1 (middle panel,
301 WT, n=7-8; Shp1, n=8-11), and relative IgG1 NP affinity (right panel, WT, n=7-8; Shp1, n=8-
302 11) at different time points post immunisation. (Results are from one to two independent
303 experiments at each time-point); horizontal lines indicate the mean. *P < 0.05, **P < 0.01,
304 ***P < 0.001, ****P < 0.0001 (parametric two-tailed unpaired t-test and two-way ANOVA).

305 **Supplementary Figure 1. GC-associated PCs during the GC response to SRBCs.**

306 Quantification of IRF4⁺ PCs from Cγ1^{Cre/+}Ptpn6^{fl/wt} (*fl/wt*) and Cγ1^{Cre/+}Ptpn6^{fl/fl} (*fl/fl*) mice d5
307 post SRBC immunisation in the GC-T zone interface (Zhang et al., 2018). Spleens were stained
308 with IRF4 (red), IgD (green), and CD4 (blue). T, T zone; GC, germinal centre. Bar, 100 μm.
309 (% of GC area; results are representative of one of two independent experiments. WT, n=4;
310 Shp1, n=5). Horizontal lines indicate the mean.

311 **Supplementary Figure 2. SHP-1 expression is decreased in GC B cells from**

312 **Cγ1^{Cre/+}Ptpn6^{fl/fl} mice.** Cγ1^{Cre/+}Ptpn6^{fl/wt} (*fl/wt*) and Cγ1^{Cre/+}Ptpn6^{fl/fl} (*fl/fl*) mice were
313 immunised with SRBCs (A) or NP-CGG (B) and SHP-1 expression was determined 5 or 8 days
314 post immunisation, respectively. Representative FACS plot (left) and summary data (right) of
315 SHP-1 expression (MFI of GC B cells; results are representative of one of two independent
316 experiments. WT, n=5; Shp1, n=5); horizontal lines indicate the mean. *P < 0.05, **P < 0.01
317 (parametric two-tailed unpaired t-test).

318 **Supplementary Figure 3. NP specific GC B cells are reduced in the absence of CSK**

319 Cγ1^{Cre/+}Csk^{fl/wt} (open blue circles) and Cγ1^{Cre/+}Csk^{fl/fl} (open red circles) mice were immunised
320 with NP-CGG and GC response was analysed 8 and 14 days post immunisation. (% of live
321 cells; results are combined from two to three independent experiments. WT, n=7-12; Shp1,
322 n=9-13); horizontal lines indicate the mean. *P < 0.05, **P < 0.01 (two-way ANOVA).

323 **Methods**

324 **RESOURCE AVAILABILITY**

325 **Lead Contact**

326 Further information and requests for resources and reagents should be directed to and will be
327 fulfilled by Lead Contact, Kai-Michael Toellner (k.m.toellner@bham.ac.uk).

328 **Materials Availability**

329 Materials generated in this study are available upon request.

330 **Data and Code Availability**

331 This study did not generate any unique datasets or code.

332 **EXPERIMENTAL MODEL AND SUBJECT DETAILS**

333 **Mice**

334 $C\gamma 1^{Cre/+} Ptpn6^{fl/wt}$ ($Shp1^{fl/wt}$) and $C\gamma 1^{Cre/+} Ptpn6^{fl/fl}$ ($Shp1^{fl/fl}$) mice were generated by the mating
335 of $C\gamma 1^{Cre/+}$ (kindly donated by S Casola, IFOM, Milan, Italy) (Casola et al., 2006) and $Ptpn6^{fl/wt}$
336 animals (Pao et al., 2007). $Ptpn6^{fl/wt}$ animals had been backcrossed extensively onto C57BL6.
337 For some experiments, $C\gamma 1^{Cre/+} Ptpn6^{fl/wt}$ mice were crossed with $ROSA^{mT/mG}$ animals
338 (007576; Jackson Laboratory), which contain a Cre-inducible membrane-tagged version of
339 eGFP (Muzumdar et al., 2007). Animal experiments were licensed by the UK Home Office
340 according to the Animals Scientific Procedures Act 1986 and approved by local ethics
341 committee, University of Birmingham, UK.

342 **METHOD DETAILS**

343 **Immunisation**

344 2×10^8 sheep red blood cells (SRBCs) (TCS Biosciences, UK) in PBS were injected
345 intravenously in the lateral tail vein. NP (4-hydroxy-3-nitrophenyl acetyl) was conjugated to
346 CGG (Chicken γ -globulin) at a ratio of NP₁₈-CGG. Mice were immunised intraperitoneally
347 (i.p.) with 50 μ g NP₁₈-CGG precipitated in alum plus 10^5 chemically inactivated *Bordetella*
348 *pertussis* (LEE laboratories, BC, USA) or subcutaneously on the plantar surface of the foot
349 with 20 μ g NP₁₈-CGG precipitated in alum plus 10^5 chemically inactivated *Bordetella pertussis*.

350 **Immunofluorescence**

351 Spleens and popliteal lymph nodes obtained at different time-points post-immunisation were
352 frozen and cryosectioned. Slides were rehydrated in PBS and blocked using 1% BSA (Sigma-
353 Aldrich) in PBS for 30 min. Antibodies were diluted at the optimal dilution in PBS, 1% BSA
354 and incubated in a humid dark chamber for 1 h. Allophycocyanin-CD4 (GK1.5),
355 BrilliantViolet421-IgD (11-26c.2a), Alexa633-goat anti-IgG1, goat anti-mouse IRF4 (M-17),
356 rabbit anti-mouse active Caspase 3 (C92-605), and sheep anti-IgD (Abcam) were used.
357 Secondary antibodies were Cy3-conjugated donkey anti-rabbit and Alexa488-conjugated
358 donkey anti-sheep, Alexa555-conjugated donkey anti-goat and streptavidin Alexa555-
359 conjugated. Slides were mounted in ProLong Gold antifade reagent (Invitrogen, UK) and left
360 to dry in a dark chamber for 24 h. Images were taken on an Axio Scan Z1 microscope (Zeiss).
361 Image data were processed using FIJI (Schindelin et al., 2012) or ZEN (Carl Zeiss Germany).

362 **Flow Cytometry**

363 Red blood cells were or not lysed by ACK lysing buffer (Gibco). Cell suspensions were
364 blocked by CD16/32 (93) diluted in FACS buffer (PBS supplemented with 0.5% BSA plus
365 2mM EDTA), and then followed with staining cocktail: BrilliantViolet510 B220 (RA3-6B2),
366 BrilliantViolet711 CD138 (281-2), NP- Phycoerythrin for detecting antigen specific B cells (in
367 house), Fluorescein isothiocyanate CD38 (90), BrilliantViolet605 Fas (Jo2), Allophycocyanin
368 IgG1 (X56), Phycoerythrin IgM (Igh-6b), rabbit anti-mouse active caspase 3 (C92-605),
369 streptavidin-Texas Red Phycoerythrin, Phycoerythrin pSYK (I120-722), monoclonal-rabbit
370 anti-SHP-1 (C14H6). Swine anti-rabbit biotin to detect rabbit anti-mouse active caspase 3.
371 Annexin V apoptosis detection kit was used for staining apoptotic and dead cells. For
372 intracellular/intranuclear staining, after surface staining, cell suspensions were treated with the
373 Foxp3/Transcription Factor Fixation/Permeabilization Foxp3 kit (eBioscience, Carlsbad, CA),

374 according to manufacturer specification. Samples were acquired using BD LSRFortessa
375 Analyzer (BD Biosciences, USA) with the software BD FACSDiva (BD Biosciences). Data
376 were analysed with FlowJo v10 (FlowJo LLC, USA).

377 **ELISA**

378 Serial dilutions of serum samples were analysed by ELISA on NP₁₅-BSA (5 µg/ml)-coupled
379 microtiter plates to detect NP-specific IgG1, or NP₂-BSA (5 µg/ml)-coupled microtiter plates
380 to measure the NP-specific IgM or the high-affinity fraction of IgG1. AP-conjugated secondary
381 antibodies anti-IgM and anti-IgG1 were from Southern Biotech. The substrate of AP was p-
382 nitrophenyl phosphate dissolved in Tris buffer (SIGMAFAST, Sigma-Aldrich). The
383 absorbance was read at 405 nm by using a Synergy HT Microplate Reader (BioTek). OD values
384 were plotted against dilution and smoothed lines were drawn through each dilution series.
385 Relative antibody titres were read as maximal dilution where OD was above an arbitrary
386 threshold. Relative affinity was calculated by dividing ELISA titre derived from NP₂-BSA-
387 coupled plates by ELISA titre derived from NP₁₅-BSA-coupled plates.

388 **Statistical analysis**

389 All analysis was performed using GraphPad Prism 7 software. To calculate significance
390 parametric two-tailed unpaired t-test and two-way ANOVA were used. Statistics throughout
391 were performed by comparing pooled data obtained from all independent experiments. P values
392 <0.05 were considered significant (*). *p<0.05, ** p< 0.01, *** p<0.001, ****p<0.0001.

393 **References**

394 Adachi, T., Wienands, J., Wakabayashi, C., Yakura, H., Reth, M., and Tsubata, T. (2001). SHP-1 requires
395 inhibitory co-receptors to down-modulate B cell antigen receptor-mediated phosphorylation of
396 cellular substrates. *J Biol Chem* 276, 26648-26655.
397 Akkaya, M., Traba, J., Roesler, A.S., Miozzo, P., Akkaya, B., Theall, B.P., Sohn, H., Pena, M., Smelkinson,
398 M., Kabat, J., *et al.* (2018). Second signals rescue B cells from activation-induced mitochondrial
399 dysfunction and death. *Nat Immunol.*

400 Bachmann, M.F., Kundig, T.M., Odermatt, B., Hengartner, H., and Zinkernagel, R.M. (1994). Free
401 recirculation of memory B cells versus antigen-dependent differentiation to antibody-forming cells. *J*
402 *Immunol* *153*, 3386-3397.

403 Buchner, M., and Muschen, M. (2014). Targeting the B-cell receptor signaling pathway in B lymphoid
404 malignancies. *Curr Opin Hematol* *21*, 341-349.

405 Calado, D.P., Sasaki, Y., Godinho, S.A., Pellerin, A., Kochert, K., Sleckman, B.P., de Alboran, I.M., Janz,
406 M., Rodig, S., and Rajewsky, K. (2012). The cell-cycle regulator c-Myc is essential for the formation and
407 maintenance of germinal centers. *Nat Immunol* *13*, 1092-1100.

408 Cariappa, A., Tang, M., Parng, C., Nebelitskiy, E., Carroll, M., Georgopoulos, K., and Pillai, S. (2001). The
409 follicular versus marginal zone B lymphocyte cell fate decision is regulated by Aiolos, Btk, and CD21.
410 *Immunity* *14*, 603-615.

411 Casola, S., Cattoretti, G., Uyttersprot, N., Koralov, S.B., Seagal, J., Hao, Z., Waisman, A., Egert, A.,
412 Ghitza, D., and Rajewsky, K. (2006). Tracking germinal center B cells expressing germ-line
413 immunoglobulin gamma1 transcripts by conditional gene targeting. *Proc Natl Acad Sci U S A* *103*, 7396-
414 7401.

415 D'Ambrosio, D., Hippen, K.L., Minskoff, S.A., Mellman, I., Pani, G., Siminovitch, K.A., and Cambier, J.C.
416 (1995). Recruitment and activation of PTP1C in negative regulation of antigen receptor signaling by Fc
417 gamma RIIb1. *Science* *268*, 293-297.

418 Dal Porto, J.M., Haberman, A.M., Kelsoe, G., and Shlomchik, M.J. (2002). Very low affinity B cells form
419 germinal centers, become memory B cells, and participate in secondary immune responses when
420 higher affinity competition is reduced. *J Exp Med* *195*, 1215-1221.

421 Davidzohn, N., Biram, A., Stoler-Barak, L., Grenov, A., Dassa, B., and Shulman, Z. (2020). Syk
422 degradation restrains plasma cell formation and promotes zonal transitions in germinal centers. *J Exp*
423 *Med* *217*.

424 de Vinuesa, C.G., Cook, M.C., Ball, J., Drew, M., Sunners, Y., Cascalho, M., Wabl, M., Klaus, G.G., and
425 MacLennan, I.C. (2000). Germinal centers without T cells. *J Exp Med* *191*, 485-494.

426 Dominguez-Sola, D., Victora, G.D., Ying, C.Y., Phan, R.T., Saito, M., Nussenzweig, M.C., and Dalla-
427 Favera, R. (2012). The proto-oncogene MYC is required for selection in the germinal center and cyclic
428 reentry. *Nat Immunol* *13*, 1083-1091.

429 Gitlin, A.D., Mayer, C.T., Oliveira, T.Y., Shulman, Z., Jones, M.J., Koren, A., and Nussenzweig, M.C.
430 (2015). HUMORAL IMMUNITY. T cell help controls the speed of the cell cycle in germinal center B cells.
431 *Science* *349*, 643-646.

432 Goodnow, C.C., Crosbie, J., Jorgensen, H., Brink, R.A., and Basten, A. (1989). Induction of self-tolerance
433 in mature peripheral B lymphocytes. *Nature* *342*, 385-391.

434 Hanayama, R., Tanaka, M., Miyasaka, K., Aozasa, K., Koike, M., Uchiyama, Y., and Nagata, S. (2004).
435 Autoimmune disease and impaired uptake of apoptotic cells in MFG-E8-deficient mice. *Science* *304*,
436 1147-1150.

437 Khalil, A.M., Cambier, J.C., and Shlomchik, M.J. (2012). B cell receptor signal transduction in the GC is
438 short-circuited by high phosphatase activity. *Science* *336*, 1178-1181.

439 Kouskoff, V., Famiglietti, S., Lacaud, G., Lang, P., Rider, J.E., Kay, B.K., Cambier, J.C., and Nemazee, D.
440 (1998). Antigens varying in affinity for the B cell receptor induce differential B lymphocyte responses.
441 *J Exp Med* *188*, 1453-1464.

442 Kraus, M., Alimzhanov, M.B., Rajewsky, N., and Rajewsky, K. (2004). Survival of resting mature B
443 lymphocytes depends on BCR signaling via the Igalphabeta heterodimer. *Cell* *117*, 787-800.

444 Lam, K.P., Kuhn, R., and Rajewsky, K. (1997). In vivo ablation of surface immunoglobulin on mature B
445 cells by inducible gene targeting results in rapid cell death. *Cell* *90*, 1073-1083.

446 Li, Y.F., Xu, S., Ou, X., and Lam, K.P. (2014). Shp1 signalling is required to establish the long-lived bone
447 marrow plasma cell pool. *Nat Commun* *5*, 4273.

448 Luo, W., Weisel, F., and Shlomchik, M.J. (2018). B Cell Receptor and CD40 Signaling Are Rewired for
449 Synergistic Induction of the c-Myc Transcription Factor in Germinal Center B Cells. *Immunity* *48*, 313-
450 326 e315.

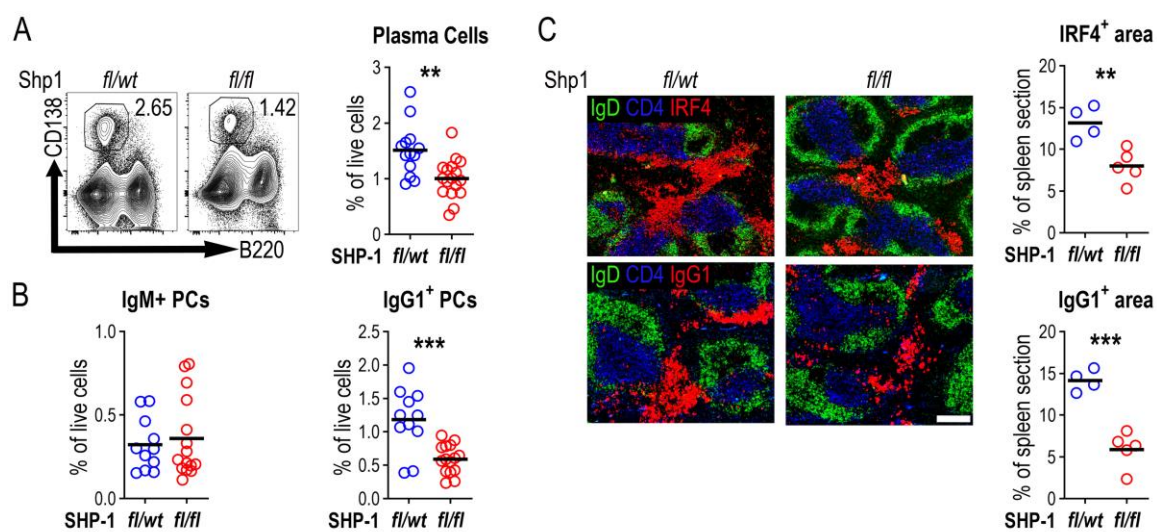
- 451 MacLennan, I.C. (1994). Germinal centers. *Annu Rev Immunol* *12*, 117-139.
- 452 MacLennan, I.C., Toellner, K.M., Cunningham, A.F., Serre, K., Sze, D.M., Zuniga, E., Cook, M.C., and
453 Vinuesa, C.G. (2003). Extrafollicular antibody responses. *Immunol Rev* *194*, 8-18.
- 454 Maeda, A., Kurosaki, M., Ono, M., Takai, T., and Kurosaki, T. (1998). Requirement of SH2-containing
455 protein tyrosine phosphatases SHP-1 and SHP-2 for paired immunoglobulin-like receptor B (PIR-B)-
456 mediated inhibitory signal. *J Exp Med* *187*, 1355-1360.
- 457 Marshall, J.L., Zhang, Y., Pallan, L., Hsu, M.C., Khan, M., Cunningham, A.F., MacLennan, I.C., and
458 Toellner, K.M. (2011). Early B blasts acquire a capacity for Ig class switch recombination that is lost as
459 they become plasmablasts. *Eur J Immunol* *41*, 3506-3512.
- 460 Mueller, J., Matloubian, M., and Zikherman, J. (2015). Cutting edge: An in vivo reporter reveals active
461 B cell receptor signaling in the germinal center. *J Immunol* *194*, 2993-2997.
- 462 Muzumdar, M.D., Tasic, B., Miyamichi, K., Li, L., and Luo, L. (2007). A global double-fluorescent Cre
463 reporter mouse. *Genesis* *45*, 593-605.
- 464 Nguyen, T.T., Klasener, K., Zurn, C., Castillo, P.A., Brust-Mascher, I., Imai, D.M., Bevins, C.L., Reardon,
465 C., Reth, M., and Baumgarth, N. (2017). The IgM receptor FcμR limits tonic BCR signaling by
466 regulating expression of the IgM BCR. *Nat Immunol* *18*, 321-333.
- 467 Niiron, H., and Clark, E.A. (2002). Regulation of B-cell fate by antigen-receptor signals. *Nat Rev Immunol*
468 *2*, 945-956.
- 469 Nitschke, L., and Tsubata, T. (2004). Molecular interactions regulate BCR signal inhibition by CD22 and
470 CD72. *Trends Immunol* *25*, 543-550.
- 471 O'Connor, B.P., Vogel, L.A., Zhang, W., Loo, W., Shnider, D., Lind, E.F., Ratliff, M., Noelle, R.J., and
472 Erickson, L.D. (2006). Imprinting the fate of antigen-reactive B cells through the affinity of the B cell
473 receptor. *J Immunol* *177*, 7723-7732.
- 474 Oropallo, M.A., and Cerutti, A. (2014). Germinal center reaction: antigen affinity and presentation
475 explain it all. *Trends Immunol* *35*, 287-289.
- 476 Pao, L.I., Lam, K.P., Henderson, J.M., Kutok, J.L., Alimzhanov, M., Nitschke, L., Thomas, M.L., Neel, B.G.,
477 and Rajewsky, K. (2007). B cell-specific deletion of protein-tyrosine phosphatase Shp1 promotes B-1a
478 cell development and causes systemic autoimmunity. *Immunity* *27*, 35-48.
- 479 Parry, S.L., Hasbold, J., Holman, M., and Klaus, G.G. (1994). Hypercross-linking surface IgM or IgD
480 receptors on mature B cells induces apoptosis that is reversed by costimulation with IL-4 and anti-
481 CD40. *J Immunol* *152*, 2821-2829.
- 482 Paus, D., Phan, T.G., Chan, T.D., Gardam, S., Basten, A., and Brink, R. (2006). Antigen recognition
483 strength regulates the choice between extrafollicular plasma cell and germinal center B cell
484 differentiation. *J Exp Med* *203*, 1081-1091.
- 485 Roco, J.A., Mesin, L., Binder, S.C., Nefzger, C., Gonzalez-Figueroa, P., Canete, P.F., Ellyard, J., Shen, Q.,
486 Robert, P.A., Cappello, J., *et al.* (2019). Class-Switch Recombination Occurs Infrequently in Germinal
487 Centers. *Immunity* *51*, 337-350 e337.
- 488 Russell, D.M., Dembic, Z., Morahan, G., Miller, J.F., Burki, K., and Nemazee, D. (1991). Peripheral
489 deletion of self-reactive B cells. *Nature* *354*, 308-311.
- 490 Schindelin, J., Arganda-Carreras, I., Frise, E., Kaynig, V., Longair, M., Pietzsch, T., Preibisch, S., Rueden,
491 C., Saalfeld, S., Schmid, B., *et al.* (2012). Fiji: an open-source platform for biological-image analysis. *Nat*
492 *Methods* *9*, 676-682.
- 493 Schwickert, T.A., Victora, G.D., Fooksman, D.R., Kamphorst, A.O., Mugnier, M.R., Gitlin, A.D., Dustin,
494 M.L., and Nussenzweig, M.C. (2011). A dynamic T cell-limited checkpoint regulates affinity-dependent
495 B cell entry into the germinal center. *J Exp Med* *208*, 1243-1252.
- 496 Shulman, Z., Gitlin, A.D., Targ, S., Jankovic, M., Pasqual, G., Nussenzweig, M.C., and Victora, G.D.
497 (2013). T follicular helper cell dynamics in germinal centers. *Science* *341*, 673-677.
- 498 Steinhoff, U., Muller, U., Schertler, A., Hengartner, H., Aguet, M., and Zinkernagel, R.M. (1995).
499 Antiviral protection by vesicular stomatitis virus-specific antibodies in alpha/beta interferon receptor-
500 deficient mice. *J Virol* *69*, 2153-2158.

- 501 Stewart, I., Radtke, D., Phillips, B., McGowan, S.J., and Bannard, O. (2018). Germinal Center B Cells
502 Replace Their Antigen Receptors in Dark Zones and Fail Light Zone Entry when Immunoglobulin Gene
503 Mutations are Damaging. *Immunity* 49, 477-489 e477.
- 504 Toellner, K.M., Luther, S.A., Sze, D.M., Choy, R.K., Taylor, D.R., MacLennan, I.C., and Acha-Orbea, H.
505 (1998). T helper 1 (Th1) and Th2 characteristics start to develop during T cell priming and are
506 associated with an immediate ability to induce immunoglobulin class switching. *J Exp Med* 187, 1193-
507 1204.
- 508 Toellner, K.M., Sze, D.M., and Zhang, Y. (2018). What Are the Primary Limitations in B-Cell Affinity
509 Maturation, and How Much Affinity Maturation Can We Drive with Vaccination? A Role for Antibody
510 Feedback. *Cold Spring Harb Perspect Biol* 10.
- 511 Tsiantoulas, D., Kiss, M., Bartolini-Gritti, B., Bergthaler, A., Mallat, Z., Jumaa, H., and Binder, C.J. (2017).
512 Secreted IgM deficiency leads to increased BCR signaling that results in abnormal splenic B cell
513 development. *Sci Rep* 7, 3540.
- 514 Tsubata, T., Murakami, M., and Honjo, T. (1994a). Antigen-receptor cross-linking induces peritoneal
515 B-cell apoptosis in normal but not autoimmunity-prone mice. *Curr Biol* 4, 8-17.
- 516 Tsubata, T., Murakami, M., Nisitani, S., and Honjo, T. (1994b). Molecular mechanisms for B lymphocyte
517 selection: induction and regulation of antigen-receptor-mediated apoptosis of mature B cells in
518 normal mice and their defect in autoimmunity-prone mice. *Philos Trans R Soc Lond B Biol Sci* 345, 297-
519 301.
- 520 Victora, G.D., and Nussenzweig, M.C. (2012). Germinal centers. *Annu Rev Immunol* 30, 429-457.
- 521 Victora, G.D., Schwickert, T.A., Fooksman, D.R., Kamphorst, A.O., Meyer-Hermann, M., Dustin, M.L.,
522 and Nussenzweig, M.C. (2010). Germinal center dynamics revealed by multiphoton microscopy with a
523 photoactivatable fluorescent reporter. *Cell* 143, 592-605.
- 524 Watanabe, N., Nomura, T., Takai, T., Chiba, T., Honjo, T., and Tsubata, T. (1998). Antigen receptor
525 cross-linking by anti-immunoglobulin antibodies coupled to cell surface membrane induces rapid
526 apoptosis of normal spleen B cells. *Scand J Immunol* 47, 541-547.
- 527 Weisel, F.J., Zuccarino-Catania, G.V., Chikina, M., and Shlomchik, M.J. (2016). A Temporal Switch in the
528 Germinal Center Determines Differential Output of Memory B and Plasma Cells. *Immunity* 44, 116-
529 130.
- 530 Yam-Puc, J.C., Zhang, L., Zhang, Y., and Toellner, K.M. (2018). Role of B-cell receptors for B-cell
531 development and antigen-induced differentiation. *F1000Res* 7, 429.
- 532 Zhang, Y., Garcia-Ibanez, L., and Toellner, K.M. (2016). Regulation of germinal center B-cell
533 differentiation. *Immunol Rev* 270, 8-19.
- 534 Zhang, Y., Tech, L., George, L.A., Acs, A., Durrett, R.E., Hess, H., Walker, L.S.K., Tarlinton, D.M., Fletcher,
535 A.L., Hauser, A.E., *et al.* (2018). Plasma cell output from germinal centers is regulated by signals from
536 Tfh and stromal cells. *J Exp Med* 215, 1227-1243.

537

538

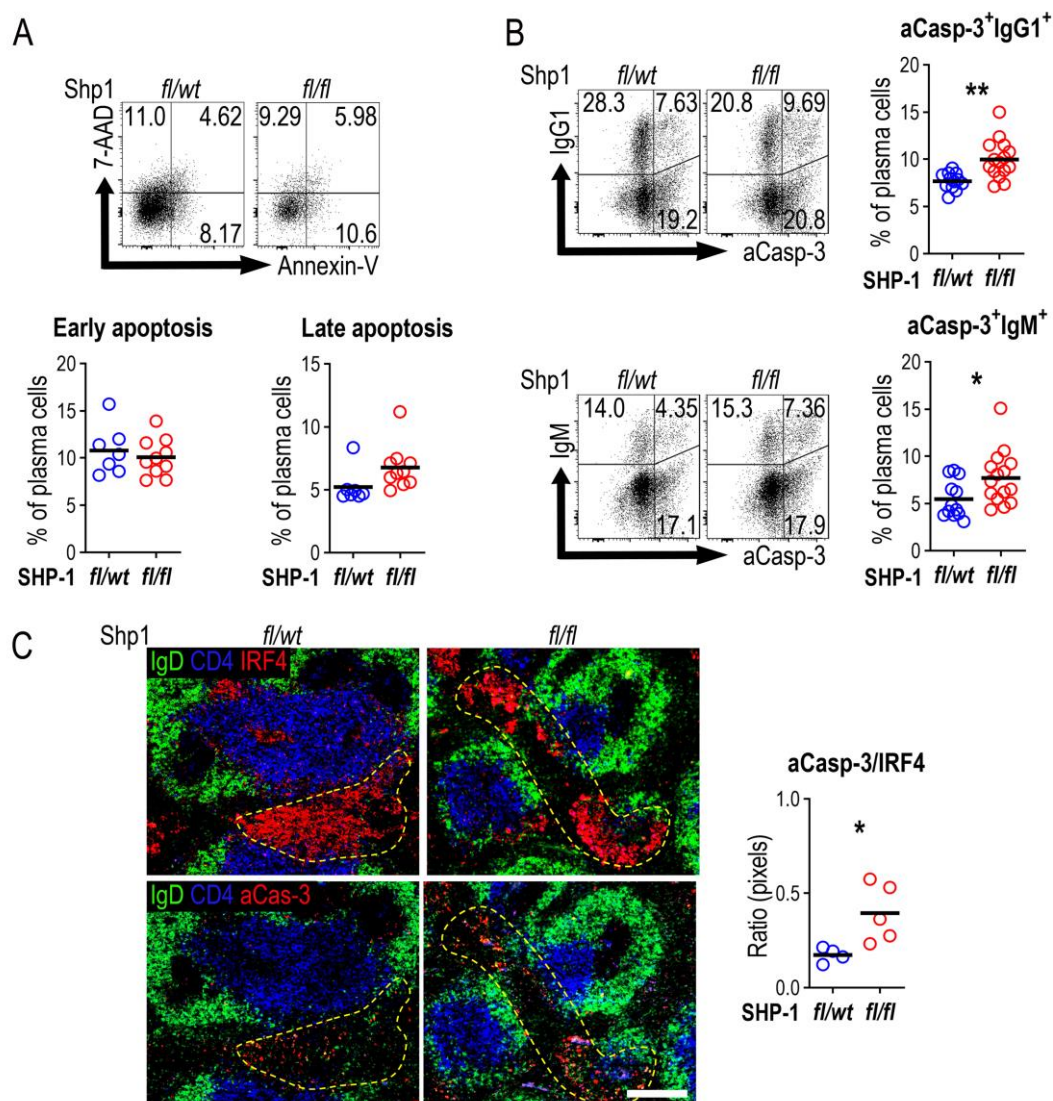
539 Figure 1.



540

541

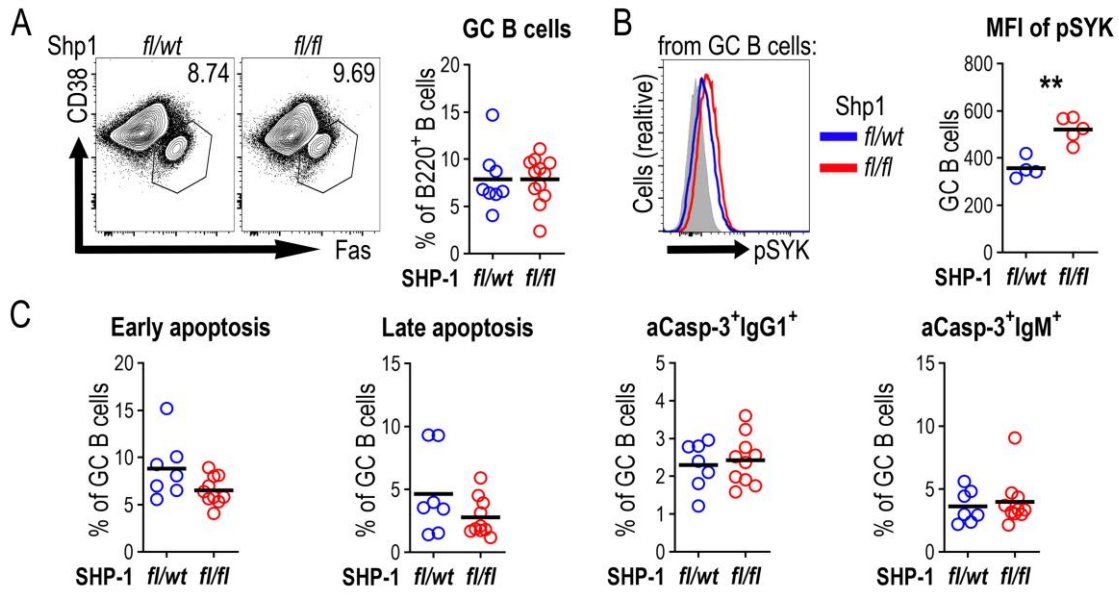
542 Figure 2.



543

544

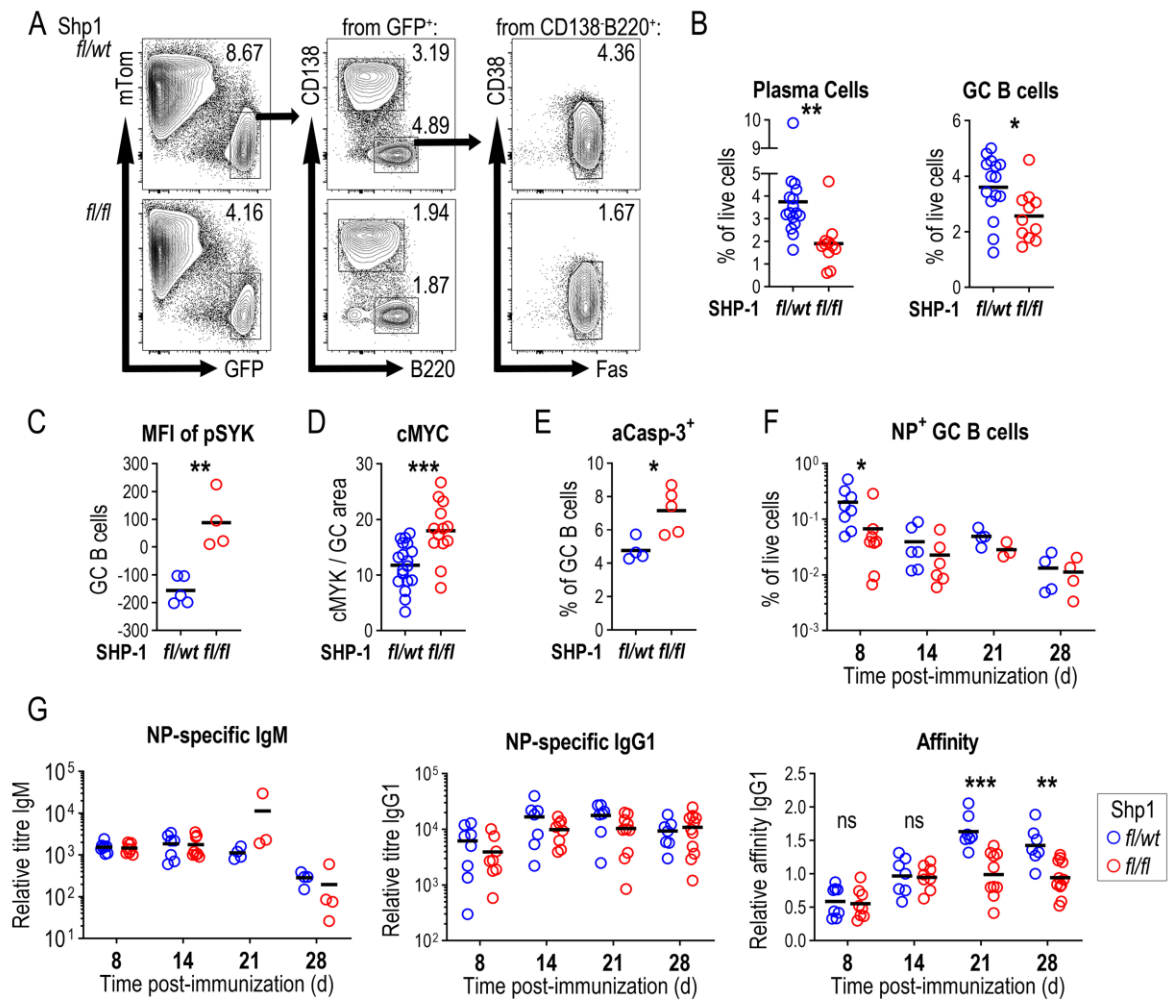
545 Figure 3.



546

547

548 Figure 4.



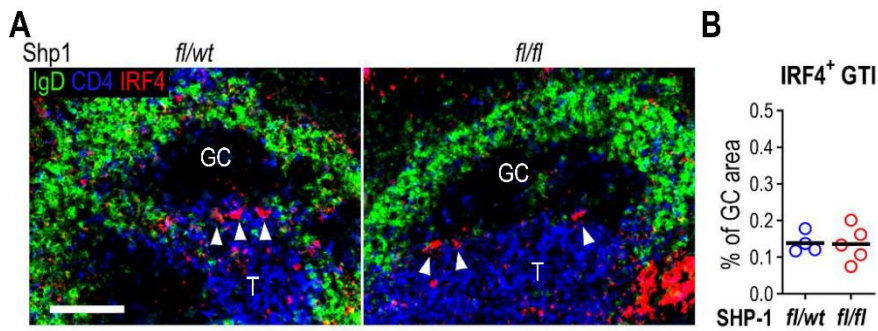
549

550

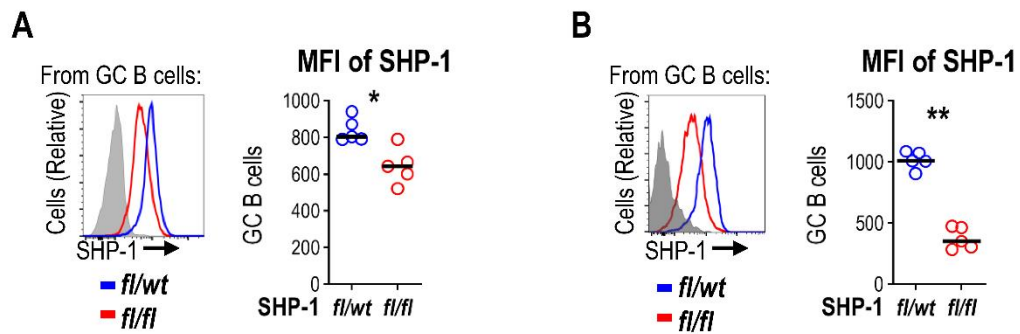
551 Supplemental material

552

553 **Supp. Fig. 1**



Supp. Fig. 2



Supp. Fig. 3

